Materials Chemistry and Physics 290 (2022) 126620

Contents lists available at ScienceDirect

Materials Chemistry and Physics

journal homepage: www.elsevier.com/locate/matchemphys

Nickel electrodeposition in LEU metal foil annular targets to produce Mo-99

Ricardo F. Ianelli *, Adonis M. Saliba-Silva, Eriki M. Takara, José Garcia Neto, José A.B. Souza, Elita F. Urano de Carvalho, Michelangelo Durazzo

Nuclear and Energy Research Institute, IPEN-CNEN/SP, São Paulo, Brazil

HIGHLIGHTS

- - Electroplating 12 μm layer of nickel on uranium metal foil target.
- - Electrodeposition of tube-shaped uranium thin foil with automated apparatus.
- - Good nickel layer adherence in uranium with surface sanding. Uranium loss of 0.16 wt%.
- - Easy assembly of uranium foil annular target with nickel electroplated layer.

GRAPHICAL ABSTRACT

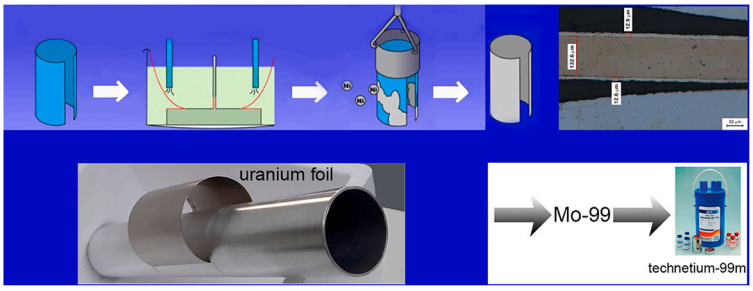

ARTICLE INFO

Keywords:
Uranium foil targets
Mo-99
Electrodeposition
Nickel
Uranium metal
Annular targets

ABSTRACT

The most used production route of Mo-99 is through the fission of U-235 in irradiation targets that are irradiated in research reactors. The annular target is a promisor design since it can incorporate high U-235 quantities, thus increasing the production yield of Mo-99. This target type uses a foil of uranium metal enveloped by a thin nickel foil that acts as a diffusion barrier. The process of uranium enveloping with nickel foil is today done manually. This operation risks the nickel foil breaking up during target assembling. In the present work, we studied the nickel electrodeposition over uranium metal foil surfaces to replace nickel foils. A pre-forming procedure of the uranium metal foil by calendering was developed to facilitate the assembling operation. The electrodeposition was done over the uranium foil pre-conformed in a tubular shape. An automated apparatus for electrodeposition of nickel in uranium tubular-shaped foil was developed. The results showed that the high nickel adherence to uranium metal depends on the proper activation of the uranium surface. Among the activation processes studied, the mechanical activation showed good adhesion of the nickel layer, with a loss of only 0.16% of uranium mass. Homogeneous and regular 12 μm thickness electrodeposited layers over the uranium metal were obtained. This work showed that the process could be used in continuous production technology, such as the production of irradiation targets.

1. Introduction

The most used radioisotope in medicinal diagnostics is the metastable technetium-99 (Tc-99 m). This isotope has been used for over 50 years, and it is present in over 80% of nuclear imaging diagnoses worldwide [1]. It has been used in about 30–40 million nuclear

* Corresponding author. Av. Prof. Lineu Prestes, 2242, Cidade Universitária, CEP 05508-000, São Paulo, SP, Brazil.
E-mail address: rfi933@hotmail.com (R.F. Ianelli).

https://doi.org/10.1016/j.matchemphys.2022.126620
Received 29 September 2021; Received in revised form 6 May 2022; Accepted 30 July 2022
Available online 4 August 2022

Table 1
Solutions and conditions of the studied activation treatments.

Activation	Solution	Concentration	Current	Time	Reference
1	No activation	N.A.	N.A.	N.A.	N.A
2	$NiCl_2.6H_20$ HNO_3	2.4 M 7.2 M	N.A.	1 min	Cieszykowska et al. [22] Petit et al. [24]
3	H_3PO_4 H_2SO_4	4.8 M 9.3 M	3A cathodic	4 min	Kočik et al. [39] Zaki [40]
4	H_3PO_4 H_2SO_4	4.8 M 9.3 M	80 mA/ cm^2	1 min	Kočik et al. [36]
5	$C_2HCl_3O_2$ HCl	0.8 M 0.7 M	80 mA/ cm^2	1 min	Rebol et al. [25] Gore et al. [26]
6	H_3PO_4 HCl	7.7 M 0.8 M	80 mA/ cm^2	1 min	Owen et al. [27] Worthington et al. [28] Gore et al. [26]
7	H_2SO_4 HCl	7.2 M 0.8 M	80 mA/ cm^2	1 min	Lundquist et al. [29,30]
8	Sanding HNO_3	Grit 400 15.6 M	N.A.	1 min	Wu et al. [32] Tang et al. [31]

N.A. = Not Applicable.

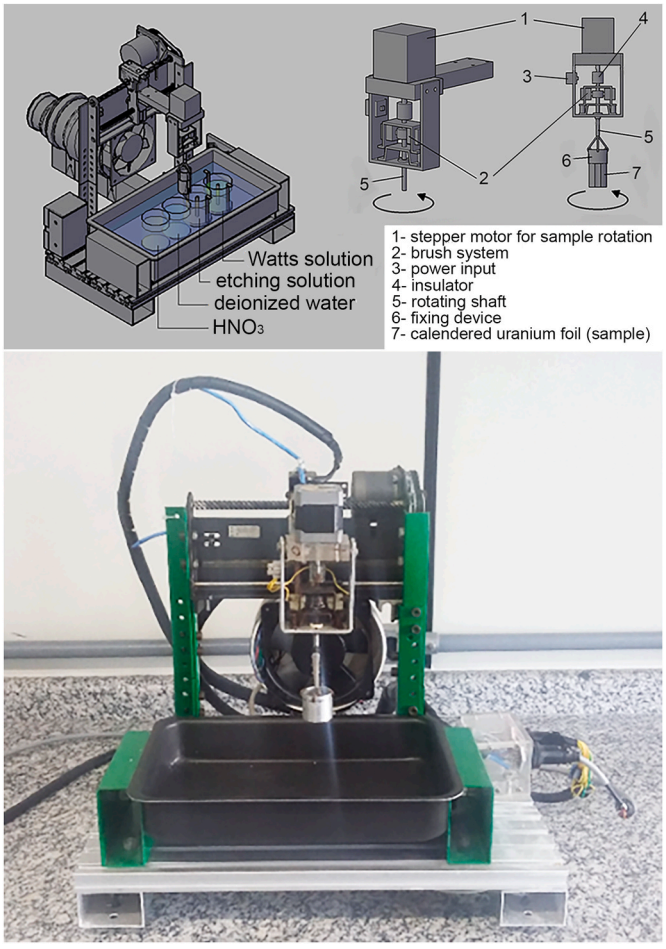

Fig. 1. Equipment for nickel electrodeposition on tubular thin uranium foil.

medicine procedures annually, and new applications have been developed for using the Tc-99 m every year [2]. It is primarily used in tomographic imaging techniques to diagnose heart and brain disease and track cancer spreading [3]. Due to its short half-life (6 h), Tc-99 m needs to reach the final consumer in the form of its parent isotope, molybdenum-99 (Mo-99), inside lyophilized cases. Valuable information on the global production, use, and projected demand of Tc-99 m is available in a report published by the U.S. National Academies of Sciences, Engineering, and Medicine [4].

The most productive method to obtain Mo-99 on an industrial scale is by fissioning U-235 through neutron irradiation of uranium-containing targets in research reactors. Uranium is incorporated into so-called irradiation targets, irradiated for about a week, and dissolved to extract Mo-99 [5].

The production of Mo-99 has been done using highly enriched uranium (HEU, > 93% U-235) to maximize the production yield. However, since 1986 the U.S. Reduced Enrichment for Research and Test Reactor Program (RERTR) has directed its studies to replace the use of HEU with low enriched uranium (LEU, < 20% U-235) in the production of 99-Mo [6,7]. Hansell [8] deals with the risks of nuclear terrorism associated with the Mo-99 production. For this reason, the international producers of Mo-99 are trying to replace conventional HEU targets with LEU.

The effort to reduce uranium enrichment resulted in developing a new type of target that uses a thin foil of LEU [9,10], produced from hot and cold rolling of uranium metal until reaching about 125 μm thickness. The uranium foil obtained is placed onto a recess machined on an aluminum tube (inner tube). The inner tube containing the uranium foil is inserted into another aluminum tube (outer tube). The assembly is inserted into a steel die, and a "draw plug" operation plastically deforms the inner tube. In this operation, the spaces between the tubes are eliminated (or reduced) to guarantee good contact that ensures the proper cooling of the target during fission. The assembly is then sealed by welding the target ends to prevent contamination of the reactor environment. After irradiation, the target is disassembled, removing the uranium foil, which is then chemically processed to recover Mo-99. The procedures for fabricating and processing the uranium metal foil annular target are available [10–15]. Vandegrift et al. [13] provide a rich background on the development of uranium metal annular targets. Due to the high density of uranium metal (around 19 g/cm^3), this type of target can compensate for the decrease in U-235 content due to the use of LEU.

The uranium foil must be protected with a diffusion barrier to prevent bonding between the uranium foil and the aluminum tube caused by the fission products. This protection is necessary to ensure easy target disassembly and extraction of the uranium foil after irradiation. Usually, this operation is carried out by enveloping the uranium foil with a thin nickel foil, which acts as a barrier to the diffusion of fission products. The recoil range of the fission fragments defines the necessary thickness of the nickel layer to be effective as a diffusion barrier. The maximum recoil distance for nickel is about 7 μm [16–18]. To prevent the bonding of the uranium foil with the aluminum tubes, a diffusion barrier layer approximately 10 μm thick was successfully used [13,14,19,20]. However, to provide a safety margin, the thickness usually adopted for the nickel layer is approximately double the recoil distance.

Although the use of nickel foils as a diffusion barrier is an effective solution to prevent diffusion between the uranium foil and aluminum tubes [12,13,21], this practice has shown that due to its small thickness, the nickel foil may break during the insertion of the inner tube into the outer tube. During insertion into the outer tube, the uranium foil wrapped with nickel must be manually positioned around the inner tube only by using the pressure exerted by the operator's fingers. This operation is delicate due to the small gap between the inner and outer tubes.

To minimize this problem, Durazzo et al. [11] developed an innovative method for target assembling. The uranium foil is pre-shaped by calendering, acquiring a tubular shape with a diameter slightly smaller than the diameter of the inner tube. In this way, the foil is perfectly fixed over the inner tube surface by itself, using its elastic force without pressure from the operator's fingers. Thus, the inner tube containing the uranium/nickel foil slides easily into the outer tube, facilitating the

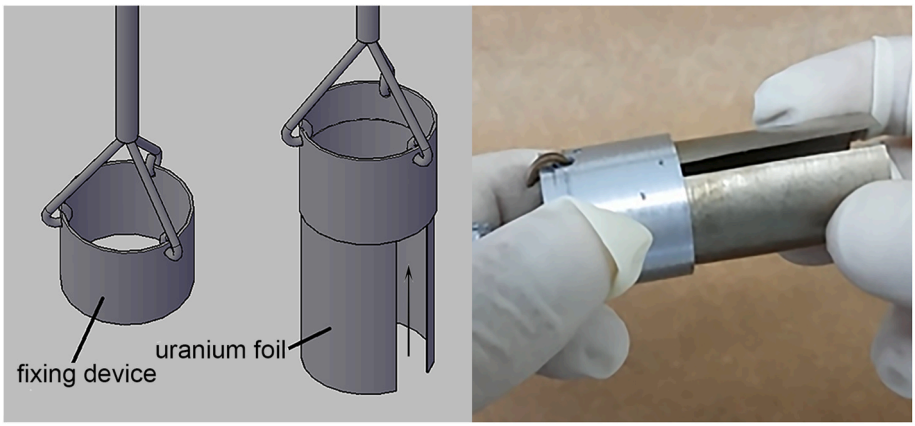

Fig. 2. Schematic attachment of the uranium foil into the fixing device.

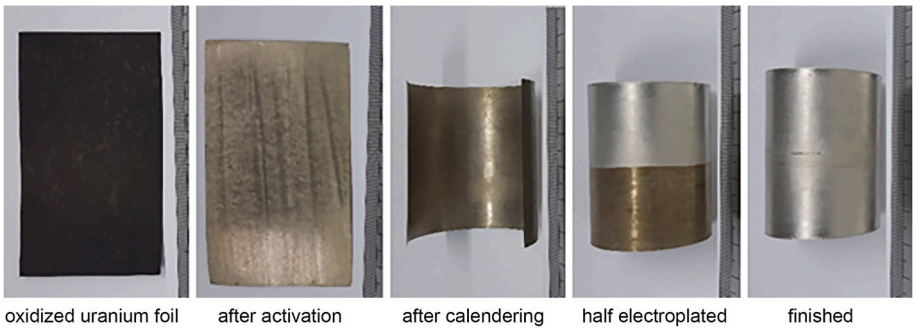

Fig. 3. The illustrative sequence of the nickel electrodeposition process on the uranium foil.

Table 2
Loss of mass in the activation treatments tested.

Activation	Solution	Type	Weight Before (g)	Weight After (g)	Weight loss (%)
1	No Activation	N.A.	N.A.	N.A.	N.A.
2	$NiCl_2.6H_20$ HNO_3	Chemical	0.6016	0.5899	1.9448
3	H_3PO_4 H_2SO_4	Cathodic	0.6405	0.6403	0.0312
4	H_3PO_4 H_2SO_4	Anodic	0.6209	0.6118	1.4656
5	$C_2HCl_3O_2$ HCl	Anodic	0.6660	0.6163	7.4625
6	H_3PO_4 HCl	Anodic	0.5948	0.5563	6.4728
7	H_2SO_4 HCl	Anodic	0.5595	0.5285	5.5407
8	Sanding	Mechanical	0.6821	0.6810	0.1613

N.A. = Not Applicable.

target assembling operation.

Another approach to eliminating the problem is replacing the nickel foil wrapping technique with electrodeposition of a nickel layer over the surface of the uranium foil. In addition to avoiding the previously mentioned problems in target assembly, Smaga et al. [16] consider nickel electrodeposition the best manufacturing approach in cost and performance. Vandegrift et al. [7] agree that plating fission barriers on the uranium foil make target preparation simpler and more economical.

Few publications on nickel plating on thin uranium foils for use in targets are found in the literature, some with limited information [7,13,16–18,20,22]. In any electrodeposition process, the activation treatment is decisive for high adhesion between the deposit and the substrate. Therefore, proper surface preparation methods are required. Smaga et al. [16] concluded that the preparation of the uranium foil before electrodeposition (activation treatment) has a significant impact on the coating quality and showed that in uranium foils without any activation treatment, the nickel layer completely fails to adhere. In addition, excessive uranium mass losses associated with activation treatments have been reported, which leads to a decrease in uranium foil thickness below the specified minimum of 112 μm.

Vandegrift et al. [13] and Smaga et al. [16] used an activation treatment consisting of an initial degreasing step (xylene or tetrachlorethylene) followed by pickling in 8 M nitric acid solution for 5–10 min. The sample was then etched with a 5.33 M ferric chloride solution for 2–5 min to roughen the surface. After that, the sample was pickled again in 8 M nitric acid for 2–7 min. The uranium mass loss from etching was less than 10%. Nickel electrodeposition used a solution of nickel sulfomate ($Ni(SO_3NH_2)_2$) with the addition of nickel bromide. The pH was stabilized at 4 with the addition of boric acid. The current density was 32 mA/cm^2, maintained for 25 min. The bath temperature was held at 40 °C. The thickness of the nickel layer obtained was 10 μm, measured by microscopy.

Vandegrift et al. [7] consider surface preparation of the uranium foil to be the most challenging step in electrodeposition. This is because the foil is fragile (125–130 μm), and it is necessary to find a balance between surface roughness and foil dissolution. They used degreasing in xylene, pickling in 8 M nitric acid, etching with ferric chloride solution at 40 °C, and immersion again in 8 M nitric acid until a metallic surface was obtained. The authors deposited zinc onto a thin uranium foil 130 μm thick, and a 12 μm layer was successfully deposited. However, the loss of uranium was significant, with 25 μm of the thin foil being removed.

Cieszykowska et al. [22] agree that the nickel plating is advantageous in relation to the wrapping of the uranium foil with the nickel foil, simplifying the target assembling. The authors used four different

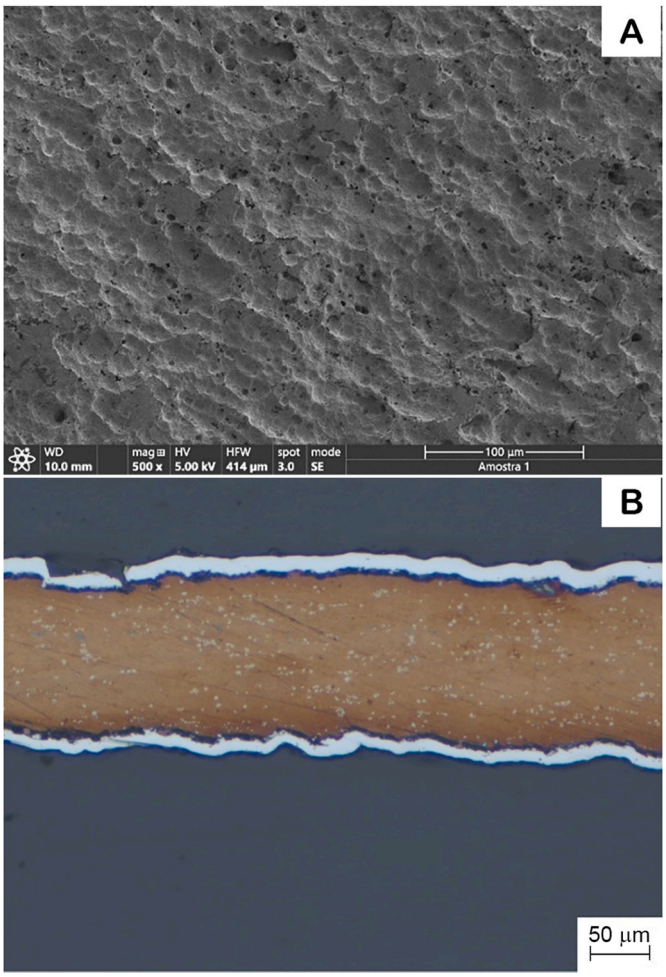

Fig. 4. Uranium foil without activation treatment. Only one pickling with HNO_3 was performed for 5 min. A –Scanning electron micrograph of the surface (secondary electrons). B – Optical micrograph of the cross-section illustrating the deposited nickel layer. A gap is observed between the nickel layer and the substrate.

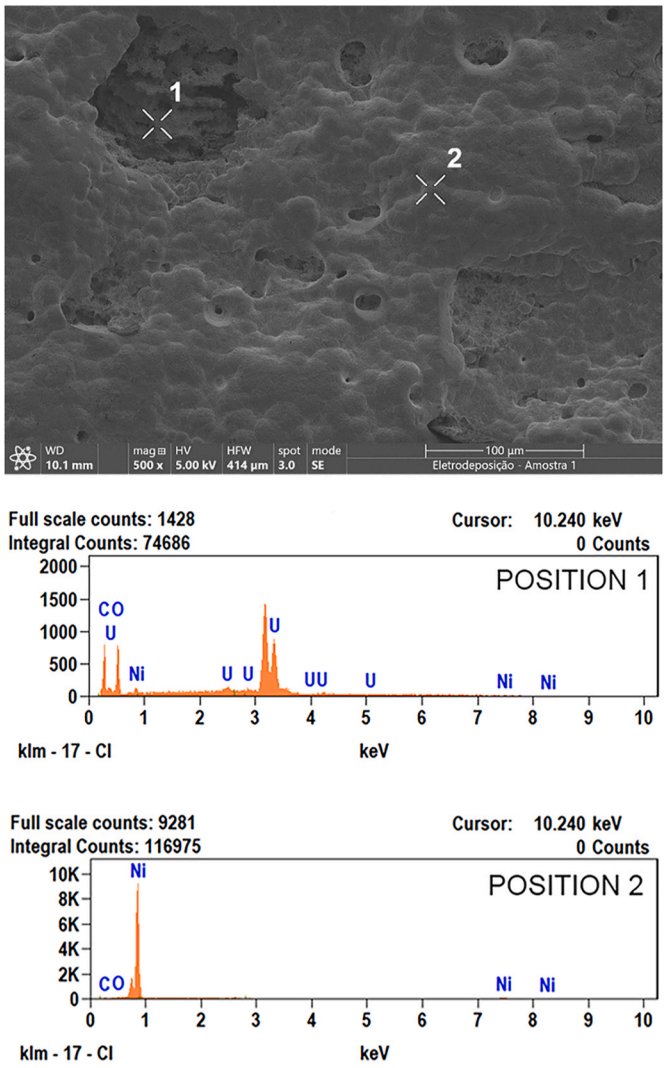

Fig. 5. Scanning electron micrograph showing discontinuity in the electrodeposited nickel layer.

methods for surface preparation prior to nickel plating. Pretreatment using a 5 M ferric chloride solution resulted in unsatisfactory results. Pretreatment using nickel chloride solution and nitric acid ($NiCl_2.6H_2O$–510 g/L + HNO_3–340 g/L) at 40 °C for 50–120 s showed promising results. Pretreatment without chloride attack, only with double pickling with 8 M nitric acid, showed good results. The Watts bath [23] (combined nickel sulfate, nickel chloride, and boric acid) was used for electrodeposition. The current density was 30 mA/cm^2, applied for 60 min at 50 °C.

Conner et al. [20] deposited nickel on uranium foil for target testing under irradiation. They obtained a 9 µm thick nickel layer using a current density of 20 mA/cm^2. Electrodeposition time was not reported. The surface pretreatment method was the same as Smaga et al. [16]. Nickel electrodeposition used a solution of nickel sulfomate (Ni$(SO_3NH_2)_2$) with the addition of nickel bromide. The uranium mass loss from etching was 5.8%.

Olivares et al. [17] and Lisboa et al. [18] electrodeposited nickel onto 120 µm thick uranium foils. The pretreatment adopted was pickling with 65% HNO_3 for 10 min. A solution of 250 g/L nickel sulfate, 60 g/L nickel chloride, and 40 g/L boric acid at 40 °C was used in the electrodeposition. Applying a current density of 3 A/cm^2 for 30 min resulted in a homogeneous nickel layer with a thickness of 32.3 µm and good adhesion.

Other activation treatments are available in published papers that studied the deposition of nickel on the surface of uranium, aiming at corrosion protection. Petit et al. [24] used trichloroethylene vapor degreasing followed by pickling in 8 N nitric acid to remove the oxide layer. Then, the surface was etched with a 2.5 M solution of nickel chloride in a 4.8 N nitric acid solution. The temperature of the solution was maintained at 42 °C. The period for the uranium attack was 50–60 s. This procedure removed approximately 18 µm from the uranium surface and produced a very clean surface for plating.

Some activation treatments adopt electrolytic attack using a solution containing chlorine ions from chlorides or hydrochloric acid together with weaker acids, such as sulfuric and phosphoric acids [25–30]. In this way, an activation effect is obtained that allows well-adhered nickel electrodeposition on the surface of the metallic uranium.

Rebol et al. [25] suggest using a solution containing from 15% to 50% by weight of trichloroacetic acid with the addition of 0.1–1% by weight of hydrochloric acid. A current density of 40–60 mA/cm^2 is applied for 3–10 min. Gore et al. [26] used a solution containing 125 g/L of trichloroacetic acid and 20 ml/L of HCl, maintaining a current density of 77 mA/cm^2 for 15 min. These authors achieved a finer roughness using a 50 v/o H_3PO_4 (85%) solution containing 20 ml/L of HCl, maintaining a current density of 77 mA/cm^2 for 10 min. Owen and Alderton [27] propose an electrolytic etching using a phosphoric acid solution with 20% by volume of hydrochloric acid, with a current density of 80 mA/cm^2 for 10 min. Worthington et al. [28] used an anodic

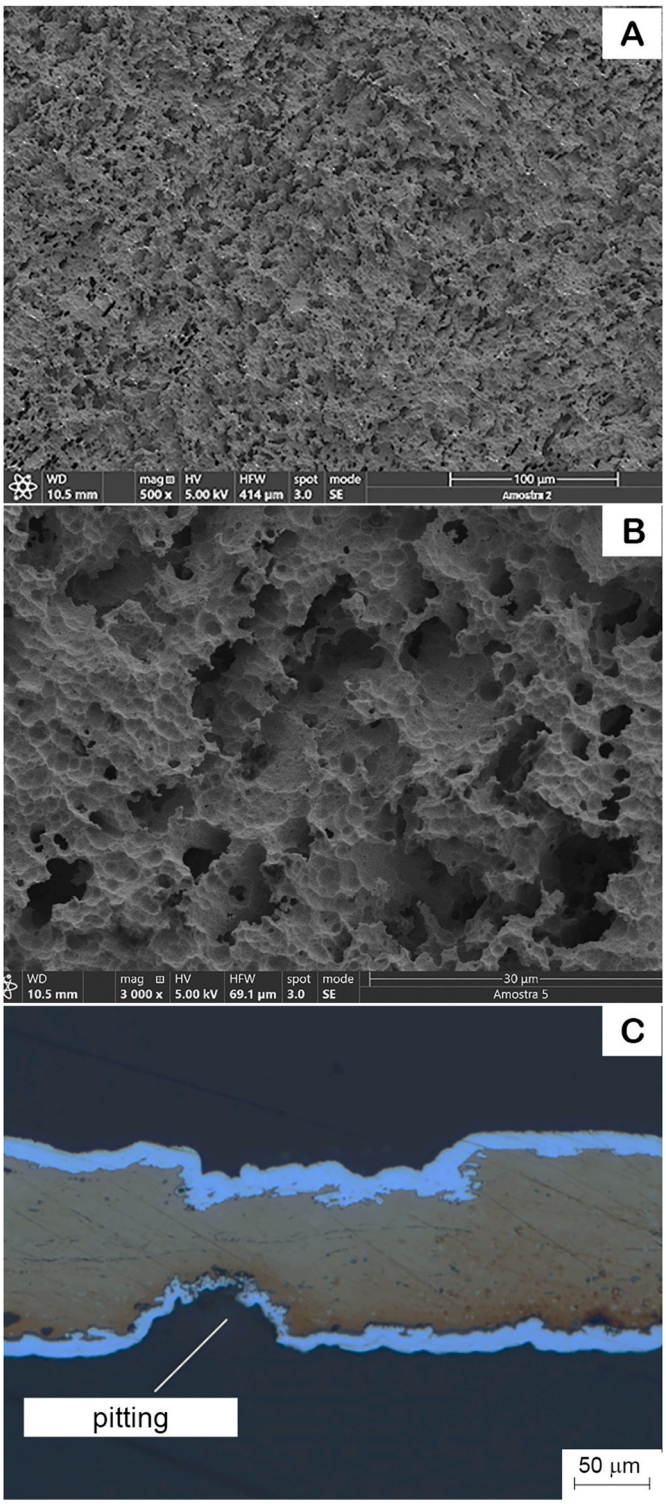

Fig. 6. Activation test 2 ($NiCl_2.6H_2O$ + HNO_3). A – Scanning electron micrograph illustrating the surface of the uranium foil (secondary electrons). B – details of A. C – Optical micrograph of the cross-section of the uranium foil. A pit is observed where the thickness of the uranium foil has been reduced to less than half. The deposited nickel layer showed good adhesion even inside the pits.

etching in a solution of 5.5 M H_3PO_4/0.2 M HCl, with a current density of 45–55 mA/cm^2 for 6–10 min. Lundquist and Stromatt [29,30] used electrolytic etching with 6 M H_2SO_4/0.32 M HCl solution, with a current density of 30–90 mA/cm^2 and etching time 3–10 min.

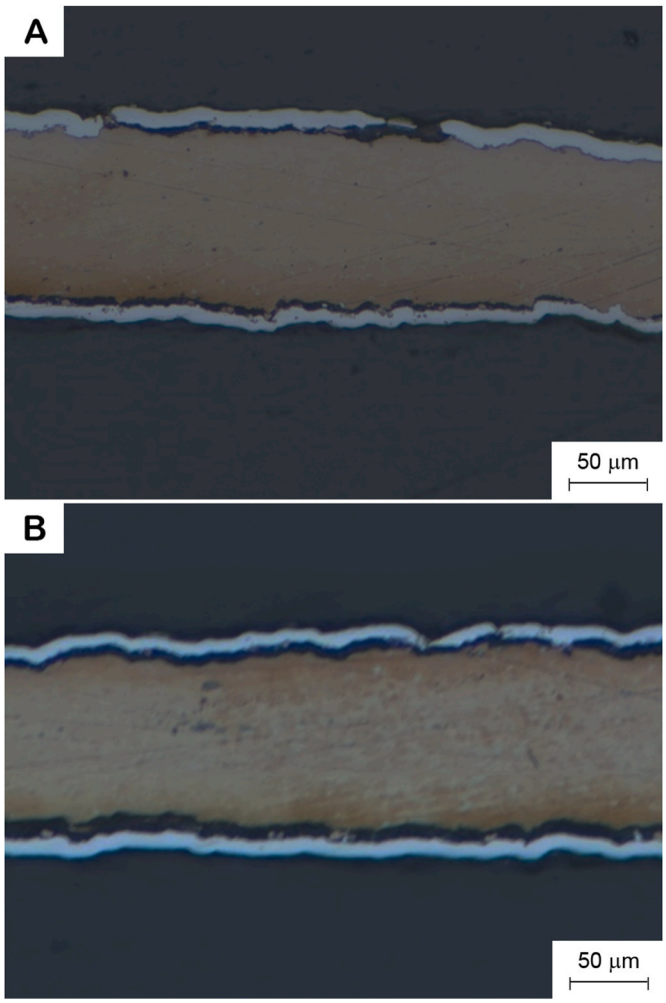

Fig. 7. Optical micrograph of the cross-section of the uranium foil subjected to: A – activation treatment 3 (H_3PO_4 + H_2SO_4 with anodic polarization). B – activation treatment 4 (H_3PO_4 + H_2SO_4 with cathodic polarization). There is a gap between the nickel layer and the substrate in both samples, demonstrating low adhesion. These results are very similar to those obtained for the sample without activation treatment (Fig. 4).

Although its use in thin uranium foils has not been found in the literature, mechanical activation treatments are also used for preparing surfaces. Materials such as superalloys form passive oxide layers on their surface quickly and reduce the adhesion ability of deposited films. Such materials require special cleaning and preparation processes for electrodeposition, which often includes mechanical activation. For example, in the deposition of palladium films on stainless steel, the activation treatment involves sanding with a SiC abrasive paper, degreasing in a basic solution, and a final step of acid activation [31]. Wu et al. [32] activate the surface of Nickel-Base Single Crystal Superalloy with SiC paper up to #600 for electroplating Pt–Ir films. Zhanwen Wang et al. [33] only use #800 sandpaper and an ultrasonic alcohol bath to prepare stainless steel samples for deposition of superhydrophobic nickel coatings. R.P. Silva et al. [34] also use sanding of the stainless steel surface with a succession of 500, 800 and 1000 grit sandpaper followed by cleaning with distilled water to electrodeposit nickel and copper. M.B. Gonzalez and S.B. Saidman [35] use 1200 grit sandpaper to prepare stainless steel samples to electroplate a polypyrrole layer as a protective oxidation layer.

In general, other complicated activation treatments are often necessary. In the electrodeposition of black nickel on copper, degreasing processes and surface activation with acids followed by the deposition of

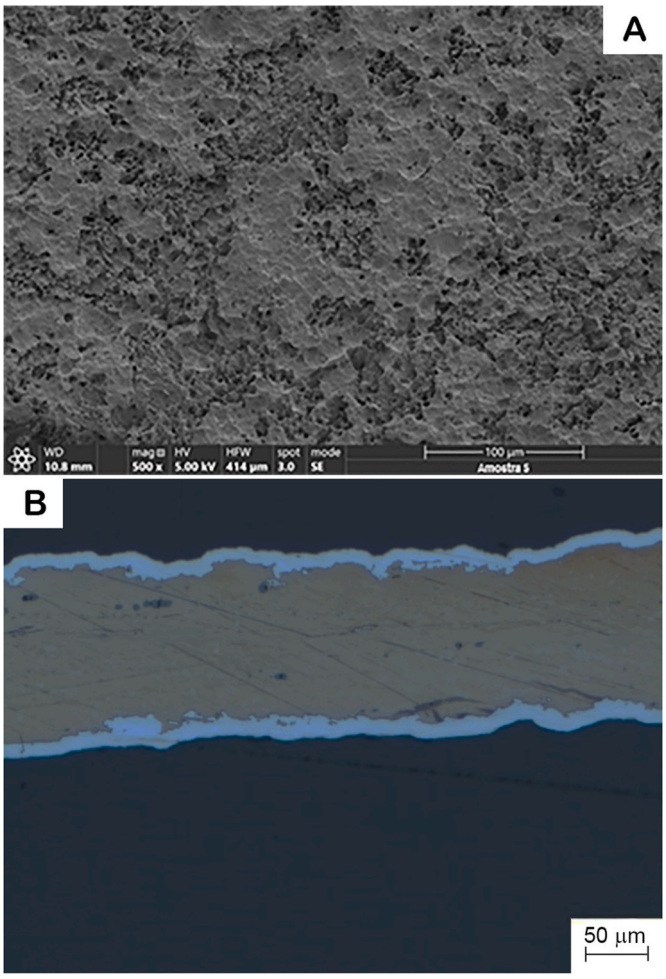

Fig. 8. Activation test 5 ($C_2HCl_3O_2$ + HCl). A – Scanning electron micrograph illustrating the surface of the uranium foil (secondary electrons). B – Optical micrograph of the cross-section of the uranium foil. Good coverage, good adhesion, and good homogeneity in the nickel layer thickness are observed.

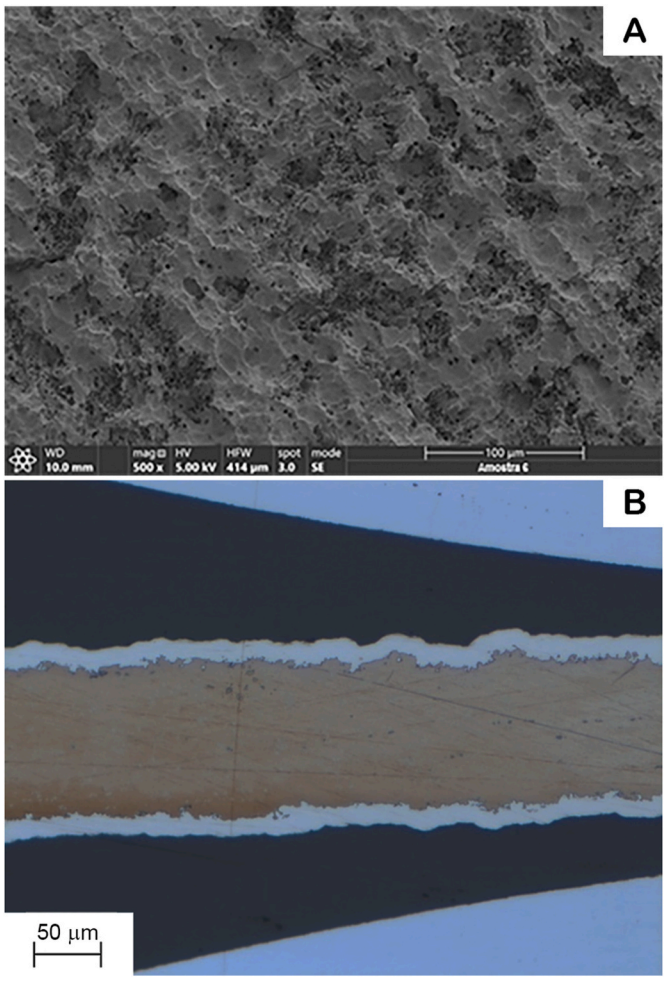

Fig. 9. Activation test 6 (H_3PO_4 + HCl). A – Scanning electron micrograph illustrating the surface of the uranium foil (secondary electrons). B – Optical micrograph of the cross-section of the uranium foil. Good coverage, good adhesion, and good homogeneity in the nickel layer thickness are observed.

a pre-layer nickel were necessary to obtain good adhesion of the black nickel layer [36]. In the deposition of palladium membranes on porous stainless steel whose substrate has a high surface roughness with large and non-uniform pores, it is necessary to form an intermediate layer that serves as an interdiffusion barrier to guarantee the formation of a deposit free of defects [37,38].

An additional difficulty in using nickel electrodeposition to apply the diffusion barrier to uranium foil targets is related to the need to deform the foils during target assembly. The nickel-covered uranium foil must be bent to be positioned in the inner tube before insertion into the outer tube at the target assembly stage. In this situation, the electrodeposited nickel layer may detach from the surface of the uranium foil. Vandegrift et al. [7] observed this problem in tests using zinc electrodeposition over uranium metal foil. These authors observed the peeling of the electrodeposited layer on the inner curvature of the uranium foil when it was bent during assembly. The detachment occurred on the side of the uranium foil where the zinc layer was being compressed. This also occurred outside the bent foil, where the zinc was tensioned but less pronounced than the compressed side.

In this work, nickel electrodeposition over uranium metal foil surfaces was studied as an alternative to nickel foil wrapping, avoiding the problem of nickel foil tearing during assembly. A novelty presented in the present work is the use of the preforming process of the thin uranium foil before nickel electrodeposition, thus avoiding the possible peeling of the electrodeposited nickel layer due to its deformation during assembly. The electrodeposition was carried out over the uranium foil already shaped in a tubular format, ready for assembling in the inner tube and, therefore, without need for its conformation after electrodeposition. As the uranium foil is already in the necessary shape, it is not necessary to apply pressure on the uranium foil covered with nickel during the target assembly, thus preventing the layer from detaching from the substrate. An apparatus was specially designed and built to carry out this task.

It is clear from the literature that for the deposited layer to have good adhesion, the uranium surface must be irregular enough so that nickel finds anchor points on the surface and can mechanically adhere to the material. The sample surfaces were previously prepared through eight different activation processes in this work. The effectiveness of the activation for forming a well-adhered electroplated nickel layer was verified employing scanning electron microscopy and optical microscopy. The balance between the roughness obtained in the activation and the dissolution of the uranium foil was evaluated by measuring the loss of mass that occurred during the activation treatment by weighing the uranium foil before and after the activation treatment.

The results demonstrated the possibility of electrodeposition of an adherent, continuous, and homogeneous nickel layer with controlled thickness over the pre-formed uranium foil in a tubular shape. No peeling of the nickel layer was observed during target assembling using uranium metal foil with electroplated nickel. A nickel layer with a thickness of around 12 µm was successfully electrodeposited.

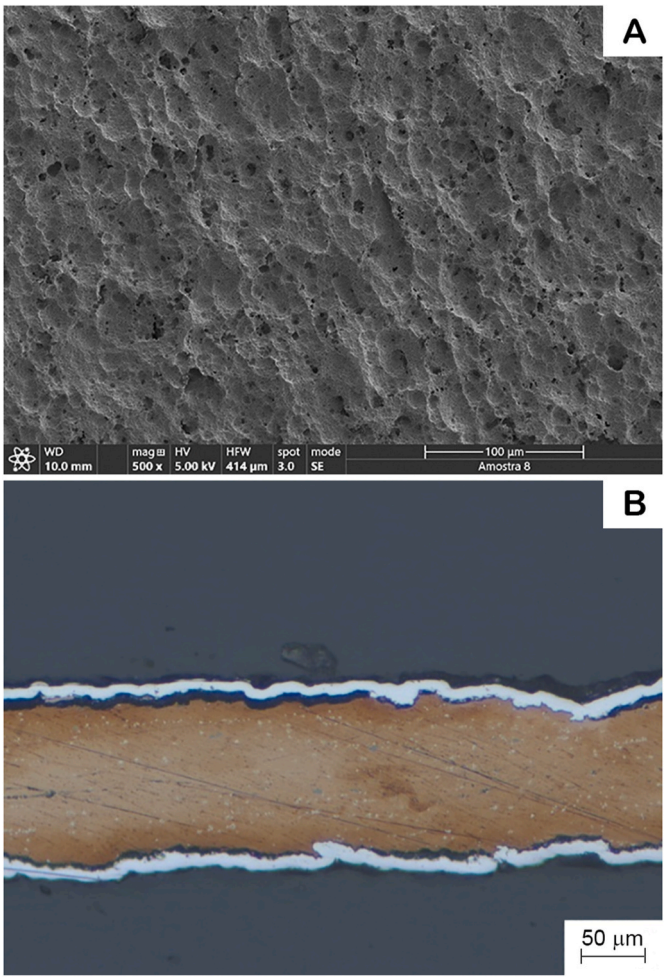

Fig. 10. Activation test 7 (H_3SO_4 + HCl). A – Scanning electron micrograph illustrating the surface of the uranium foil (secondary electrons). B – Optical micrograph of the cross-section of the uranium foil. There is good coverage but poor adhesion of the nickel layer.

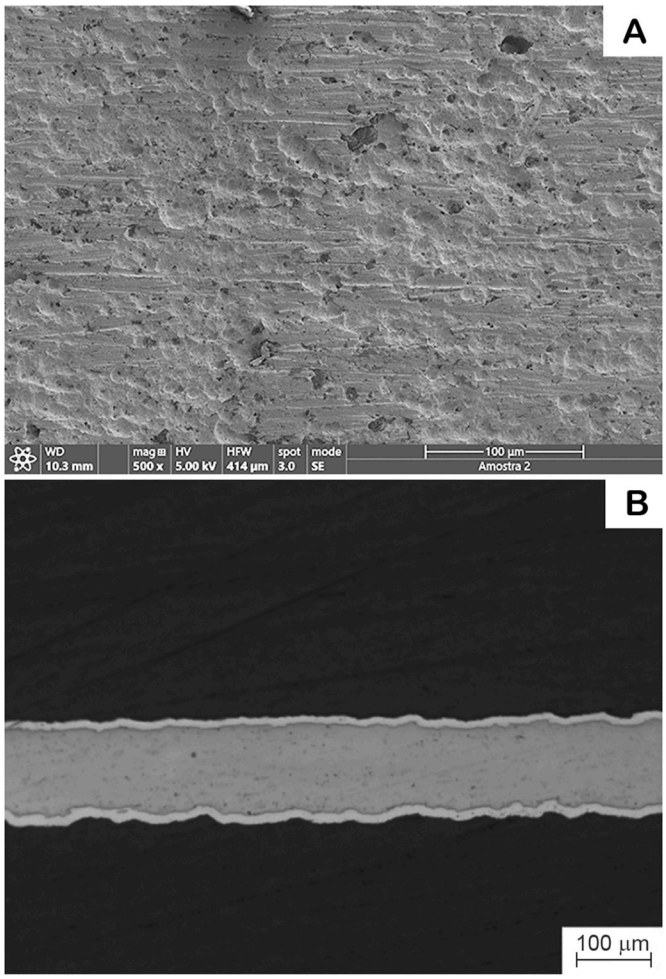

Fig. 11. Activation test 8 (sanding). A – Scanning electron micrograph illustrating the surface of the uranium foil (secondary electrons). B – Optical micrograph of the cross-section of the uranium foil. There is good coverage, good adhesion, and good homogeneity in the thickness of the nickel layer.

2. Experimental

The procedures adopted for fabricating the thin uranium metal foil and its shaping in the tubular form are described in previous work [11].

Based on methods found in the literature, different activation processes were tested, which are described in Table 1. Flat uranium foils 10 mm wide X 30 mm long X 0.125 mm thick (3 cm^2 surface area) were used for the activation tests. Before the activation treatment, all samples were degreased with acetone and immersed in a 15.6 M HNO_3 solution for 5 min to remove oxides. The activated samples were immersed in 15.6 M HNO_3 for 1 min before electrodeposition. In order to evaluate the activation treatment's efficiency, nickel electrodeposition experiments were carried out on the activated samples. Uranium mass loss was measured by weighing before and after the activation treatment.

For the electrodeposition, the Watts solution was used [23] with a composition of 240 g/L of nickel sulfate ($NiSO_4(H_2O)_6$), 40 g/L of nickel chloride ($NiCl_2$), and 30 g/L of boric acid (H_3BO_3). Boric acid was added to stabilize the pH at 4. The polarization and current control system used in the activation and electrodeposition processes was the GI21P pulse rectifier from General Inverter. The current density was the same as Smaga et al. [16], fixed at 32 mA/cm^2. All treatments were carried out at a temperature of 25 °C. The electrodeposition time was kept constant at 20 min in all experiments. This value was calculated to obtain an electroplated nickel layer with a thickness between 12 and 13 µm, assuming the cathodic efficiency of 95.5% recommended by Di Bari [23]. Vandegrift et al. [13] and Conner et al. [20] used a nickel thickness of 9 µm to prevent the uranium foil from bonding with the aluminum tubes during irradiation tests carried out in Indonesia. The results obtained in these tests showed that the uranium foil did not bond with the aluminum tubes of the target, demonstrating that a nickel layer thickness greater than 9–11 µm was sufficient to prevent this effect.

After the nickel activation and electrodeposition treatments, the surface of the samples was observed in a scanning electron microscope (SEM) coupled to a dispersive energy spectrometer (EDS) from Thermo Fisher Scientific, model Quattro ESEM. The coating quality and adhesion were examined using optical microscopy, observing the cross-section of the samples. The samples were embedded in epoxy resin and sanded with 320, 600, 800, and 1200 sandpapers. Then, the samples were polished with a diamond paste (1 µm), followed by polishing on colloidal silica (0.06 µm). The samples were observed in a Zeiss optical microscope; model Axio Imager M2m coupled to an image analyzer.

After evaluating the activation treatments efficiency on the nickel layer adherence and considering the uranium mass loss, the most suitable activation treatment was selected to be applied in the electrodeposition tests performed on samples shaped in tubular form. In this case, the uranium foils followed the same dimensions used in the target developed by the Argonne National Laboratory (ANL), reported by Vandegrift et al. (44.8 mm wide X 75.8 mm long - 34 cm^2) [13]. Electrodeposition equipment was designed and built to carry out the process with the uranium foil in a tubular format. Fig. 1 shows an illustrative

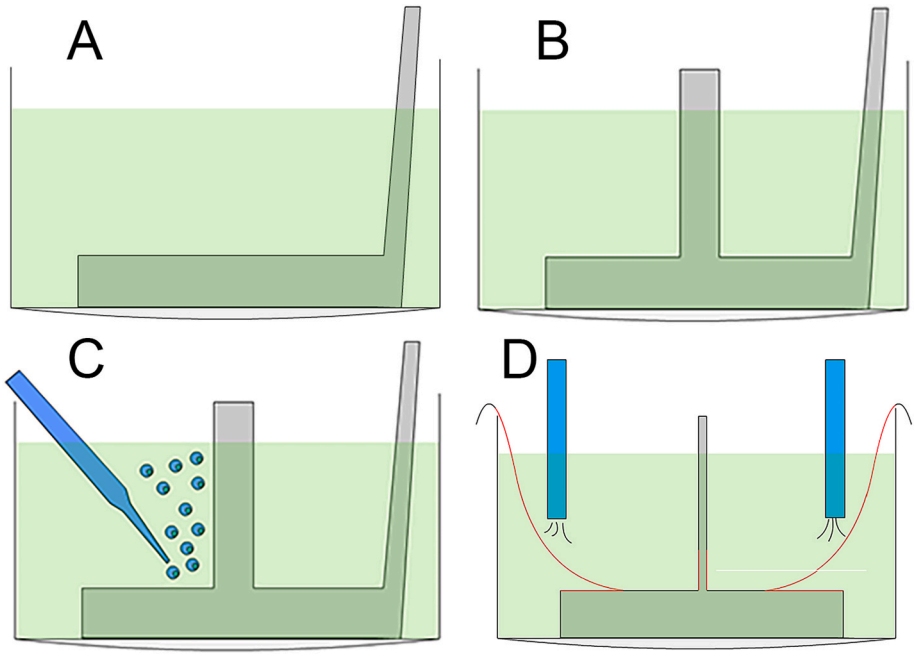

Fig. 12. Illustration of the counter electrode scheme and bath conditions used in the nickel electrodeposition tests.

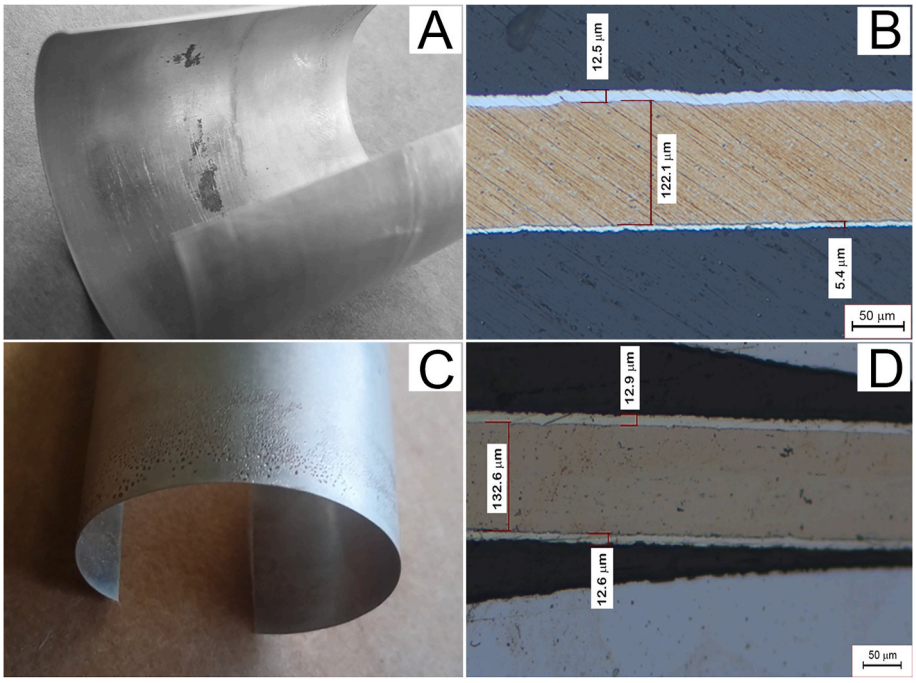

Fig. 13. Illustration of the evolution of electrodeposition as a function of the geometries shown in Fig. 12.

diagram and a picture of the equipment.

Process solutions are placed in containers inside a small tank filled with water. The main container holds the Watts solution for nickel electrodeposition. The other containers are put side by side with the activation solution, water used for washing, and the HNO_3 solution.

A direct current motor is coupled to graphite brushes connected to the electrical source and pressed against a shaft through springs, enabling the transfer of electrical current to the electrochemical processes. At the same time, the motor enables a controllable and programmable rotational movement to be applied to the tubular uranium foil through the shaft. Fig. 1 illustrates the layout of the power supply and rotation system of the uranium foil.

The tubular-shaped uranium foil is attached to the electrodeposition equipment by fitting it into a fixing device, as shown in Fig. 2. The fixing device is manufactured with a diameter slightly smaller than that of the tubular-shaped uranium foil so that it remains attached to the interior of the device by its own elastic force. This tensile strength also ensures efficient electrical contact between the fixing device and the uranium foil. The diameter of this device is 23 mm, and the diameter of the tubular uranium foil is 26 mm. The uranium foil is inserted 10 mm inside the device.

The electroplating bath (Watts solution) was stirred by recirculating

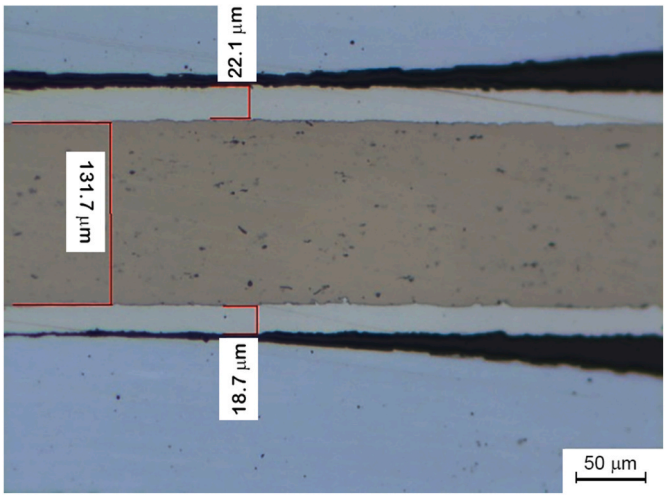

Fig. 14. Optical micrograph of the cross-section of the central region of the uranium foil (about 5.2 mm wide) illustrating the increased thickness of the nickel layer in this region.

the solution by a 0.7W hydraulic pump with a flow of 120 L/h to promote uniformity of nickel distribution in all of the foil surfaces. The equipment provides vertical and horizontal movement of the uranium foil, enabling the automatic transfer of the uranium foil between all the solutions used in the electrodeposition process and lateral agitation of the sample inside the containers. The displacement speed and positioning of the uranium foil are programmable and controlled by computer software.

After manual fixation of the uranium foil in the fixation device, the operation of the electrodeposition equipment is fully automatic, with the parameters of the entire process controlled by a computer.

Electrodeposition was performed in two steps. In the first step, the uranium foil was immersed in the bath to a height of 25 mm, and the first half of the foil was coated with nickel. Then, the target was inverted, and the uranium foil was immersed again up to a height of 25 mm, with nickel being electroplated in the second half of the foil. There was a small area in the central region of the uranium foil in which the electrodeposition was superimposed, with a width of about 5.2 mm. Fig. 3 illustrates the steps of the nickel electrodeposition process, from cleaning the oxidized uranium foil to the electrodeposition of nickel on its entire surface. After electrodeposition of the nickel layer, the uranium foil was used to assemble a target according to the procedure described in previous work [11]. The objective was to verify any difficulties caused by the electrodeposited nickel layer during the assembly.

3. Results and discussion

3.1. Activation tests

The electrodeposition equipment described early was used for the activation/electrodeposition tests. In these tests, flat samples were fixed using clamps. A nickel counter electrode coupled to the side of the container was used to deposit layers of similar thickness on both sides of the sample. The uranium foil was moved with a rotation of 20 rpm and lateral displacement movements of 1 cm each second during the process.

A problem related to activation procedures is the possibility that they cause an excessive loss of uranium and a consequent thinning of the uranium foil. Table 2 shows the mass loss resulting from the activation treatments tested.

The sample that did not receive any activation treatment (activation 1) had only its oxide layer removed with 15.6 M HNO_3 solution for 5 min. This sample had a relatively smooth surface, as shown in Fig. 4A. Although HNO_3 dissolved the uranium oxide existing on the surface of the material, the chemical attack on the metallic surface was uniform. This result was already expected because the lack of an activation

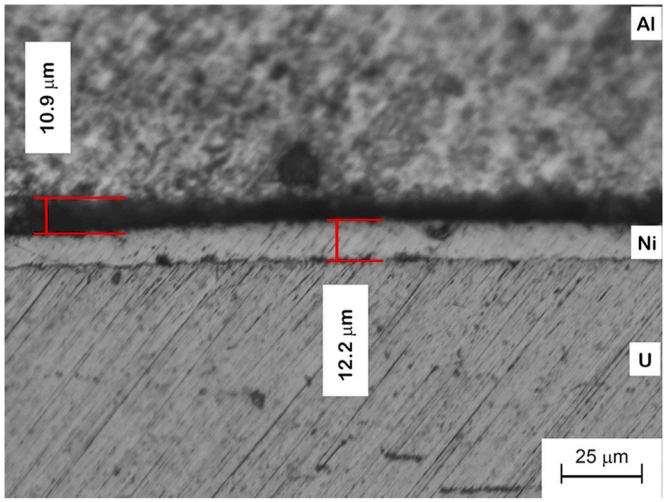

Fig. 16. Nickel layer appearance after target assembly.

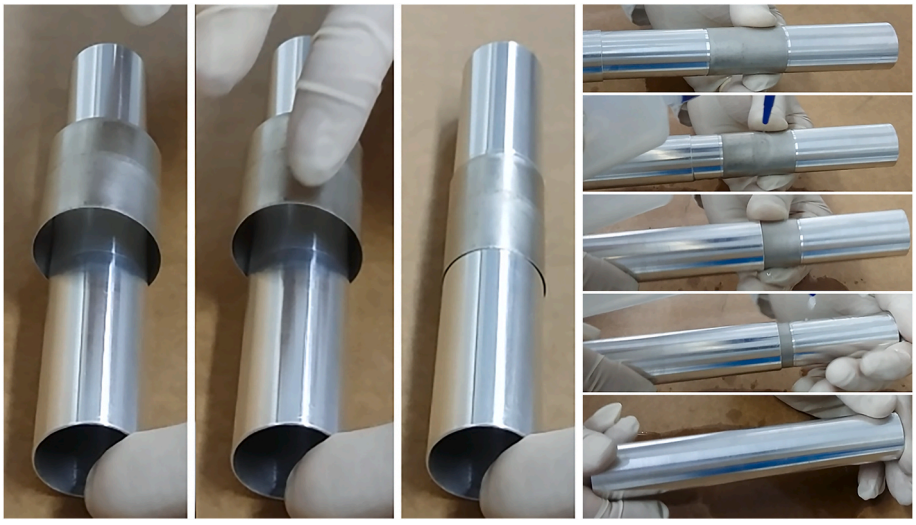

Fig. 15. Target assembly sequence with thin nickel-plated uranium foil.

treatment caused the surface of the uranium foil to show very few imperfections in which nickel could penetrate and mechanically adhere, making it difficult to attach to the surface. For this reason, the electroplated nickel layer failed to adhere to the surface of the uranium foil. A gap can be seen between the nickel layer and the uranium metal substrate, as shown in Fig. 4B. Some sites even showed peeling of the nickel layer, as shown by the EDS spectrum in Fig. 5. Uranium metal substrate without nickel coating can be seen at point 1.

In activation test 2, chloride ions promoted intense localized corrosion, resulting in deep attacks on the uranium foil surface by pitting corrosion. This activation treatment resulted in a morphology full of small pits over the entire surface of the uranium foil, as shown in Fig. 6A. Fig. 6B shows details of the pits formed on the surface.

This activation test provided a nickel layer with good adhesion. However, it formed regions with pits deep enough to cause a significant decrease in the thickness of the uranium foil, as shown in Fig. 6C. This pronounced decrease in thickness is not acceptable as it may cause insufficient heat transfer during target irradiation. Continuous contact between the uranium foil and the target's cladding tubes is essential for efficient heat exchange and target cooling in irradiation. Note that nickel penetrated the small cavities, forming a continuous layer even inside the pits.

To prevent pitting and maintain a low uranium mass loss, activation tests 3 and 4 used an electrochemical polishing solution with sulfuric acid and phosphoric acid [39]. Unlike other activation methods generally used, these activation solutions did not have chlorine ions in their composition.

In activation test 3, the sample was subjected to cathodic polarization, which inserts electrons into the cathode, causing an electrochemical reaction to reduce hydrogen ions on the metal surface [40]. In this case, hydrogen bubbles that evolve in the process mechanically clean the surface of the sample. Activation test 4 used the same activation solution proposed in activation test 3 but used anodic polarization, which is typically used in electrochemical activation processes to cause the surface imperfections necessary for the adhesion of the electrodeposited layer. Although these experiments showed the lowest mass loss among the electrochemical processes studied, the absence of chlorine ions made the surface morphology obtained in activation tests 3 and 4 very similar to the surface morphology obtained for the sample that did not undergo an activation process, shown in Fig. 4. Therefore, both tests failed to promote an adhered nickel layer over the uranium foil, as shown in the cross-section of the samples after electrodeposition illustrated in Fig. 7. The appearance of the nickel layer deposited using activation treatments 3 and 4 is very similar to that obtained in the sample that did not receive activation treatment, illustrated in Fig. 4B.

These results confirmed that the presence of chlorine was necessary for an adequate activation of the metallic uranium surface. For this reason, in the following activation tests, the samples were electrochemically activated with solutions containing hydrochloric acid (HCl) and another weak acid. Activation tests 5 and 6 used HCl and trichloroacetic acid ($C_2HCl_3O_2$) and phosphoric acid (H_3PO_4), respectively. Both activation tests resulted in very similar surfaces, with a morphology described in the literature as an "optimal activation" [26]. In this case, it is possible to observe localized regions with many indentations due to hydrochloric acid activity (similar to activation test 2, Fig. 6) distributed in the middle of regions where the surface appears unchanged, resulting from the action of weak acids. Both activations 5 and 6 provided a well-adhered nickel layer on the uranium foils. However, these two activation treatments resulted in the most significant mass loss of uranium foils, 7.4% (activation 5) and 6.7% (activation 6).

Fig. 8 shows the result obtained with the activation treatment 5, and Fig. 9 shows the result obtained with the activation treatment 6. A complete nickel coating with a very homogeneous layer thickness is observed in both cases.

In activation test 7, the action of sulfuric acid seems to have overlapped the action of hydrochloric acid, resulting in a less rough surface, with the presence of few imperfections, as shown in Fig. 10A. Consequently, despite its homogeneous thickness and continuity, the nickel layer deposited over the sample failed to adhere to the uranium surface (Fig. 10B). In addition, the mass loss resulting from this activation treatment was high, 5.5%.

As the purpose of the activation process is to create structures for the mechanical fixation of the nickel layer, in activation test 8, a simpler process was tested, which was mechanical grinding with sandpaper followed by pickling in 15.6 M HNO_3 for 1 min. Although not used for uranium, the technique of mechanical activation by sanding has already been successfully used in the electroplating process on other substrates [31,32].

This process resulted in a surface containing grooves seen in Fig. 11A. The cross-section of the sample subjected to this activation treatment (Fig. 11B) shows that the presence of these grooves was enough for the deposited nickel layer to remain adhered to the surface of the uranium foil. The nickel layer showed continuity and good homogeneity in thickness.

Among the activation tests that demonstrated good adhesion of the nickel layer to the uranium metal foil surface and continuity and homogeneity of the thickness of the deposited layer, the activation treatment 8 was the one with the lowest mass loss. This treatment also proved to be simpler to implement, as it does not require acids or electrochemical connections, avoiding the generation of liquid waste contaminated with uranium. Therefore, for its convenience, the sanding of the foil surface with 400 grit sandpaper was the activation treatment defined for carrying out nickel electrodeposition tests on tubular-shaped uranium foils.

3.2. Electrodeposition tests on tubular shaped uranium foils

Uranium metal foils manufactured according to the procedures described in previous work [11] were cut in dimensions 44.8 mm wide X 75.8 mm long (34 cm^2) and pickled in a 15.6 M HNO_3 solution for 5 min to remove the oxides. After pickling, the uranium foils were manually sanded on both sides with 400 grit sandpaper using eight passes along the entire length of the foil. Irregular movements were used to distribute the scratches over the surfaces randomly. After sanding, the foils were calendered to obtain a tubular shape. They were again pickled in the 15.6 M HNO_3 solution for 1 min to remove impurities that may have contaminated the surface of the uranium foil.

The system used for fixing the uranium foil was coupled to the electroplating machine (Fig. 2). After the activation tests, the nickel counter electrode arrangement has been modified to incorporate a base at the bottom of the container. This modification was necessary to promote the uniform distribution of the electrodeposited layer in the inner region of the tubular-shaped foil, as shown in Fig. 12A. However, the electrodeposition test using this geometry failed to deposit nickel on the inner side of the uranium foil, mainly in the central region. Parts of the uranium foil were visibly exposed (see Fig. 13 A) because the material flow tends to converge, always taking the shortest path towards the electrode to be electrodeposited. As the region inside the target is the one that presents the greatest distance in relation to the nickel counter electrode, this region received less deposition. The imagined solution to this problem was adding a pin in the center of the nickel base, as shown in Fig. 12B. In this case, the material flow lines are also routed to the interior of the sample, thus solving the problem observed.

Although this new electrode geometry eliminates the problem of lack of nickel in the inner region of the tubular-shaped uranium foil, visually covering the entire sample, the inspection by optical microscopy of the nickel layer revealed that the outer region of the uranium foil had a much thicker layer than the thickness of the layer deposited in the inner region of the sample, which had a thickness smaller than the minimum recommended by the literature (7 μm). Fig. 13 B shows this result.

The problem possibly occurred because, despite the existence of an electrode close to the inner surface of the uranium foil, the inner

electrode occupied much space in the central region of the tubular-shaped target and left little volume of solution for deposition on the inner surface of the foil. The central electrode and the target geometries made it difficult to renew the solution in this region, which was poor in nickel ions in relation to the outer region of the bath, preventing the nickel layer in the inner region from reaching the same thickness as the layer in the outer region. The rotation movement applied to the foil was not enough to promote the homogenization of the electrolytic bath. The solution was stirred through the injection of nitrogen gas directed to the interior region of the target to promote the homogenization of the concentration of the electrolyte solution and the elimination of the problem. The scheme used is illustrated in Fig. 12C. However, this method left round-shaped defects in the deposited layer, indicating that the gas bubbles injected into the solution prevented the electrodeposition of nickel on the surface of the uranium foil, as shown in Fig. 13C.

Olivares et al. [17] and Lisboa et al. [18] used recirculation of the electrochemical bath to maintain the homogeneity of the solution during the electrodeposition process. This technique was also adopted in the present work. Fig. 12D shows the new geometry used. The red lines on the nickel counter electrode indicate the regions coated with resin to balance the amount of material deposited on both sides of the tubular-shaped uranium foil. In this scheme, a central electrode of a smaller diameter was also used to allow a greater volume of solution in the region of the foil's interior and recirculation of the electrolytic bath during the electrodeposition process. Using this scheme, the tubular-shaped uranium foil's interior and exterior surfaces showed the deposition of a continuous nickel layer with good adhesion and homogeneous thickness, between 12 and 13 μm. Fig. 13 D shows the result.

As mentioned earlier, nickel electrodeposition was carried out in two steps. The first half of the uranium foil was covered, and then it was inverted, covering its second half. Therefore, in the central region of uranium foil (about 5.2 mm wide), the electrodeposition occurred in double, overlapping the layers. This situation resulted in a thicker layer thickness in this region, as shown in Fig. 14.

The results obtained in the electrodeposition tests were considered satisfactory using a central nickel counter electrode and recirculation of the electrolyte solution, according to the scheme shown in Fig. 12D. However, an increase in the nickel layer thickness deposited at the ends and in the central region (5.2 mm wide) of the tubular-shaped uranium foil was observed. For this reason, a target assembly test using the uranium foil under these conditions was carried out. The objective was to verify whether these effects could cause difficulties in assembling the target.

3.3. Target assembly using uranium foil with electroplated nickel layer

Details of the uranium thin foil annular target assembly procedure are described by Durazzo et al. [11] in an earlier publication. The only difference was replacing nickel foil that envelops the uranium foil by coating it with a nickel layer by electrodeposition.

The tubular-shaped uranium foil containing the electroplated nickel layer was placed into a machined recess in the inner tube, as illustrated in Fig. 15. The tubular shape of the uranium foil allowed fitting it around the inner tube without the need for foil deformation, preserving the integrity of the electroplated nickel layer. Next, the inner tube containing the uranium foil was inserted into the outer tube, as illustrated in Fig. 15. Both tubes were made of aluminum.

After this assembly, the set was inserted into a matrix. The inner tube was plastically deformed by the action of a "draw plug" with a diameter slightly larger than the inner diameter of the inner tube. No abnormal events were observed during the target assembly with the uranium foil electroplated with nickel. The inner tube containing the uranium foil slid smoothly into the outer tube. The nickel layer maintained its integrity during the inner tube expansion operation, the most aggressive assembling operation. Fig. 16 shows that the nickel layer remained adhered and intact after the target assembly. When using enveloped nickel foil as a diffusion barrier, it is common to observe a space between the nickel foil and the uranium foil, with a width of around 5 μm [11]. This gap was not observed using the electrodeposition process.

The gap between the nickel and the outer tube surface is unavoidable and typical in this target production process. Values between 10 and 30 μm are established as acceptable [17] and considered small enough to ensure good heat transfer during target irradiation. In the target assembly containing the electrodeposited nickel layer, the observed gap between the nickel and the aluminum tube was 10.9 μm.

4. Conclusions

The electrodeposition of a nickel layer on the metallic uranium foil was studied to eliminate the difficulties observed in the traditional target fabrication procedure, which adopts the enveloping of the uranium foil with a nickel foil to act as a diffusion barrier.

The electrochemical methods of activating uranium foil using $C_2HCl_3O_2$ + HCl and H_3PO_4 + HCl (methods 5 and 6, respectively) proved efficient, ensuring a well-adhered and uniform nickel layer. However, such methods consumed a greater amount of uranium (6.5–7.5% by mass). Activation by mechanical action (sanding) demonstrated satisfactory adhesion of the nickel layer with minimal loss of uranium mass (0.16%).

The feasibility of electrodeposition of a continuous and adherent nickel layer in both surfaces of the tubular uranium foil was demonstrated. The nickel layer thickness obtained was about 12 μm for 20 min of deposition with a current density of 32 mA/cm^2.

The behavior of the electrodeposited nickel layer during target assembly was satisfactory. No voids were observed between the nickel layer and the surface of the uranium foil after target assembling. This represents an advantage over nickel foil wrap, which results in a gap between the nickel foil and the uranium foil.

The automated electrodeposition equipment proved to effectively promote a nickel electrodeposition process on the preformed thin sheet in the tubular shape. This methodology proved to be applicable on a production scale.

Credit author statement

Ricardo F. Ianelli: Investigation, Methodology and Resources. **Adonis M. Saliba-Silva**: Writing - Review and Editing. **Eriki M. Takara:** Investigation, Methodology and Resources. **Jose S. Garcia Neto:** Investigation, Methodology and Resources. **Jose A. B. Souza:** Investigation, Resources and Data Curation. **Elita F. Urano de Carvalho:** Visualization. **Michelangelo Durazzo**: Project administration, Conceptualization, Methodology, Supervision, Validation, Funding acquisition, Writing - Original Draft and Writing- Reviewing.

Declaration of competing interest

The authors declare that they have no known competing financial interests or personal relationships that could have appeared to influence the work reported in this paper.

References

[1] S.K. Lee, G.J. Beyer, J.S. Lee, Development of industrial-scale fission 99Mo production process using low enriched uranium target, 2016, Nucl. Eng. Technol. 48 (2016) 613–623, https://doi.org/10.1016/j.net.2016.04.006.

[2] Nuclear Energy Agency, in: The Supply of Medical Radioisotopes: 2016 Medical Isotope Review: 99Mo/99mTc Market Demand and Production Capacity Projection 2016-2021, Nuclear Energy Agency, 2016. NEA/SEN/HLGMR(2016)2. (available at: Nuclear Energy Agency (NEA) - The Supply of Medical Radioisotopes: 2016 Medical Isotope Supply Review: 99Mo/99mTc Market Demand and Production Capacity Projection 2016-2021 (oecd-nea.org).

[3] R. Barnowski, Insourcing nuclear medicine, Journal of Science Policy & Governance 1 (2011) 1–4 (available at: https://www.sciencepolicyjournal.org/uploads/5/4/3/4/5434385/_insourcing_nuclear_medicine.pdf.

[4] National Academies of Sciences, Engineering, and Medicine, 2016. Molybdenum-99 for Medical Imaging, The National Academies Press, Washington DC, 2016, https://doi.org/10.17226/23563.

[5] P. Verbeek, in: Report on Molybdenum 99 Production for Nuclear Medicine 2010-2020, Association of Imaging Producers & Equipment Suppliers, 2008 (available at: https://www.oecd-nea.org/med-radio/docs/200902_AIPESMolySupplyReport.pdf.

[6] International Atomic Energy Agency, Technical Reports Series no 478, in: Feasibility of Producing Molybdenum-99 on a Small Scale Using Fission of Low Enriched Uranium or Neutron Activation of Natural Molybdenum, International Atomic Energy Agency, 2015 (available at: https://www-pub.iaea.org/MTCD/Publications/PDF/trs478web-32777845.pdf.

[7] G.F. Vandegrift, J.L. Snelgrove, S. Aase, M.M. Bretscher, B.A. Buchhoh, D. J. Chaiko, D.B. Chamberlain, L. Chen, C. Conner, D. Dong, G.L. Hofman, J. C. Hutter, G.C. Knighton, I.D. Kwok, R.A. Leonard, J.E. Matos, J. Sedlet, B. Srinivasan, W.D.E. alker, T. Wiencek, E.L. Wood, D.G. Wygmans, A. Travelli, S. Landsberger, D. Wu, A. Suripto, A. Mutalib, H. Nasution, H.G. Adang, L. Hotman, S. Almini, S. Dedi, R. Martalena, A. Gogo, B. Purwadi, D.L. Amin, A. Zahiruddin, Sukmana, Sriyono Kadarisman, D. Hafid, M. Sayadet, in: Converting Targets and Processes for Fission-Product 99Mo from High to Low-Enriched Uranium. Production Technologies for Molybdenum-99 and Technetium-99m, International Atomic Energy Agency, Vienna, Austria, 1999. IAEA-TECDOC-1065 (available at: https://inis.iaea.org/collection/NCLCollectionStore/_Public/30/013/30013596.pdf?r=1&r=1.

[8] C. Hansell, Nuclear medicine's double hazard: imperiled treatment and the risk of terrorism, Nonproliferation Rev. 15 (2008) 185–208, https://doi.org/10.1080/10736700802117270.

[9] T.C. Wiencek, G.L. Hofman, Development of uranium metal targets for 99Mo production, Japan on October 4-7, 1993, in: Proceedings of the 1993 International Meeting on Reduced Enrichment for Research and Test Reactors (RERTR) Held in Oarai, Japan Atomic Energy Research Institute, March 1994, p. 385. JAERI –M 94-042 (available at: https://www.osti.gov/servlets/purl/10189292.

[10] C. Conner, E.F. Lewandowski, J.L. Snelgrove, M.W. Liberatore, D.E. Walker, T. C. Wiencek, D.J. McGann, G.L. Hofman, G.F. Vandegrift, Development of annular targets for 99Mo production, in: Proceedings of the 1999 International Meeting on Reduced Enrichment for Research and Test Reactors (RERTR) Held in Budapest, 1999. Hungary on October 3-8, available at: https://inis.iaea.org/collection/NCLCollectionStore/_Public/35/015/35015949.pdf.

[11] M. Durazzo, J.A.B. Souza, R.F. Ianelli, E.M. Takara, J.S. Garcia Neto, A.M. Saliba-Silva, E.F. Urano de Carvalho, Manufacturing LEU-foil annular target in Brazil, Ann. Nucl. Energy 165 (2022), 108646, https://doi.org/10.1016/j.anucene.2021.108646.

[12] B. Briyatmoko, B. Guswardani, S. Purwanta, S. Permana, D. Basiran, M. Kartaman, Indonesia's current status for conversion of Mo-99 production to LEU fission, in: Proceedings of the 2007 International Meeting on Reduced Enrichment for Research and Test Reactors (RERTR) Held in Prague, 2007. Czech Republic on September 23-27, available at: http://www.rertr.anl.gov/RERTR29/index.html.

[13] G. Vandegrift, M.A. Brown, J.L. Jerden, A.V. Gelis, D.C. Stepinski, S. Wiedmeyer, A. Youker, A. Hebden, G. Solbrekken, C. Allen, D. Robertson, S. El-Gizawy, S. Govindarajan, A. Hoyer, P. Makarewics, J. Harris, B. Graybill, A. Gunn, J. Berlin, C. Bryan, S. Sherman, R. Hobbs, F. Griffin, J. Carbajo, J. Freels, D. Chandier, C. J. Hurt, P. Williams, Low-enriched Uranium High-Density Target Project: Compendium Report, Argonne National Laboratory, September, 2016. ANL/NE-16/15 (available at: https://publications.anl.gov/anlpubs/2016/11/130420.pdf.

[14] D. Wu, S. Landsberger, G.F. Vandegrift, Progress in chemical treatment of LEU targets by the modified CINTICHEM process, in: Proceedings of the 1996 International Meeting on Reduced Enrichment for Research and Test Reactors (RERTR) Held in Seoul, 1996. Korea on October 7-10, available at: http://www.rertr.anl.gov/99MO96/WU96.PDF.

[15] M.A. Brown, J.L. Jerden Jr., A.V. Gelis, D.C. Stepinski, S. Wiedmeyer, A. Youker, A. Hebden, G.F. Vandegrift, Development of frontend processing to allow use of high-density LEU foil targets in current Mo-99 production facilities, in: Proceedings of the 2014 Topical Meeting on Molybdenum-99 Technological Development Held in Washington, D.C. USA, 2014 on June 24-27, available at: http://mo99.ne.anl.gov/2014/pdfs/papers/S11P3%20Paper%20Brown.pdf.

[16] J.A. Smaga, J. Sedlet, C. Conner, M.W. Liberatore, D.E. Walker, D.G. Wygmans, G. F. Vandegrift, Electroplating fission-recoil barriers onto LEU-metal-foils for ^{99}Mo-production targets, in: Proceedings of the 1997 International Meeting on Reduced Enrichment for Research and Test Reactors (RERTR) Held in Jackson Hole, Wyoming, 1997. U.S.A. on 5-10 October, available at: https://www.rertr.anl.gov/Fuels97/JSmaga.pdf.

[17] L. Olivares, J. Lisboa, J. Marin, M. Barrera, Coating of Leu foil with electrodeposited nickel for 99Mo production, in: Proceedings of the 2015 European Research Reactor Conference (RRFM) Held in Bucharest, Romania on 19-23 April, 2015, European Nuclear Society, Brussels, Belgium, 2015, p. 370 (available at: https://inis.iaea.org/collection/NCLCollectionStore/_Public/47/116/47116398.pdf?r=1.

[18] J. Lisboa, J. Marin, M. Barrera, G. Cifuentes, Manufacturing of annular targets made of LEU foil coated with electrodeposited nickel, Procedia Mater. Sci. 8 (2015) 434–441, https://doi.org/10.1016/j.mspro.2015.04.094.

[19] A. Hoyer, An Investigative Approach to Explore Optimum Assembly Process Design for Annular Targets Carrying LEU Foil, Thesis presented to the Faculty of the Graduate School at the University of Missouri, Columbia, December 2013 (available at: https://mospace.umsystem.edu/xmlui/handle/10355/43063.

[20] C. Conner, M.W. Liberatore, A. Mutalib, J. Sedlet, D. Walker, G.F. Vandegrift, Progress in developing processes for converting 99Mo production from high- to low-enriched uranium-1998, in: Proceedings of the 1998 International Meeting on Reduced Enrichment for Research and Test Reactors (RERTR) Held in São Paulo, 1998. Brazil on October 18-23, (available at: https://www.osti.gov/etdeweb/servlets/purl/20221517.

[21] G.L. Hofman, T.C. Wiencek, E.L. Wood, J.L. Snelgrove, A. Suripto, H. Nasution, D. Lufti-Amin, A. Gogo, Irradiation tests of 99Mo isotope production targets employing uranium metal foils, in: Proceedings of the 1996 International Meeting on Reduced Enrichment for Research and Test Reactors (RERTR) Held in Seoul, 1996. Korea on October 7-10, available at: https://www.rertr.anl.gov/99MO96/GLHOF196.pdf.

[22] I. Cieszykowska, M. Żółtowska, M. Mielcarski, Electroplating nickel onto uranium as fission-recoil barrier, Nukleonika 54 (2009) 29–32 (available at:, untitled (nukleonika.pl).

[23] G.A. Di Bari, Electrodeposition of nickel, in: Modern Electroplating, John Wiley & Sons, Inc., Hoboken, NJ, USA, 2011, pp. 79–114, 2011.

[24] G.S. Petit, R.R. Wright, C.A. Kienberger, C.W. Weber, Electroless nickel plating for corrosion protection of uranium, Oak Ridge, TN (United States), K-1777 (available at: https://www.osti.gov/servlets/purl/4739685, 1969.

[25] W.E. Rebol, R. Wash, R.F. Wehrmann, Method of Electroplating on Uranum, United States Patent Office, US2884364A, 1959 (available at: https://patentimages.storage.googleapis.com/7e/14/cb/97acee3bc8cf38/US2884364.pdf.

[26] J.K. Gore, R. Seegmiller, J.M. Taub, A. Pinkerton, L. Quintana, Chemical Surface Treatments for Uranium and Their Application to Uranium Technology, Los Alamos Scientific Lab., N. Mex., 1957. LA-2190 (available at: https://www.osti.gov/servlets/purl/4340139/.

[27] L.W. Owen, J.R. Alderton, Electrodeposited nickel as a protective coating for uranium in unsaturated air near ambient temperature, Br. Corrosion J. 5 (1970) 217–226, https://doi.org/10.1179/000705970798324405.

[28] H. Worthington, J.C. Woodhouse, W.J. O'Leary, W. File, M.H. Wahl, P.H. Permar, C.C. McBride, Meeting at BMI on Electroplating Uranium for Extrusion Cladding, du Pont de Nemours & Company Report, 1956. DPW-56-405 (available at: 10177127 (osti.gov).

[29] J.R. Lundquist, R.W. Stromatt, Nickel Electroplating on Uranium: Surface Preparation and Plating Solution Studies, Batelle Memorial Institute, Richland, WA, 1965. BNWL-124 (available at: https://digital.library.unt.edu/ark:/67531/metadc1033830/m2/1/high_res_d/4563456.pdf.

[30] J.R. Lundquist, R.W. Stromatt, Method of Preparing Uranium for Nickel Plating, United States Patent Office, 1966. US3275535A, (available at: https://patents.google.com/patent/US3275535A/en.

[31] J. Tang, Z. Zhang, Y. Wang, P. Ju, Y. Tang, Y. Zuo, Y, Corrosion resistance mechanism of palladium film-plated stainless steel in boiling H2SO4 solution, 2018, Corrosion Sci. 135 (2018) 222–232, https://doi.org/10.1016/j.corsci.2018.02.055.

[32] Y. Wu, A. Suzuki, H. Murakami, S. Kuroda, Characterization of electroplated platinum–iridium alloys on the nickel-base single crystal superalloy, Mater. Trans. 46 (10) (2005) 2176–2179, https://doi.org/10.2320/matertrans.46.2176.

[33] Z. Wang, L. Shen, W. Jiang, M. Fan, D. Liu, J. Zhao, Superhydrophobic nickel coatings fabricated by scanning electrodeposition on stainless steel formed by selective laser melting, Surf. Coating. Technol. 377 (2019), 124886, https://doi.org/10.1016/j.surfcoat.2019.08.015.

[34] R.P. Silva, S. Eugénio, T.M. Silva, M.J. Carmezim, M.F. Montemor, Fabrication of three-dimensional dendritic Ni–Co films by electrodeposition on stainless steel substrates, J. Phys. Chem. C 116 (2012) 22425–22431, https://doi.org/10.1021/jp307612g.

[35] M.B. Gozález, S.B. Saidman, Electrodeposition of polypyrrole on 316L stainless steel for corrosion prevention, Corrosion Sci. 53 (1) (2011) 276–282, https://doi.org/10.1016/j.corsci.2010.09.021.

[36] S. Somasundaram, A.M. Pillai, A. Rajendra, P. Aravindram, P.M. Krishna, A. K Sharma, A. K, Space qualification and characterization of high emittance black nickel coating on copper and stainless steel substrates, 2018, Sol. Energy Mater. Sol. Cell. 174 (2018) 163–171, https://doi.org/10.1016/j.solmat.2017.08.023.

[37] A.D. Kiadehi, M. Taghizadeh, Fabrication, characterization, and application of palladium composite membrane on porous stainless steel substrate with NaY zeolite as an intermediate layer for hydrogen purification, Int. J. Hydrogen Energy 44 (5) (2019) 2889–2904, https://doi.org/10.1016/j.ijhydene.2018.12.058.

[38] B.S. Seo, J.Y. Han, K.Y. Lee, D.W. Kim, S.K. Ryi, S. K, Electroless Pd deposition on a planar porous stainless steel substrate using newly developed plating rig and agitating water bath, 2017, Kor. J. Chem. Eng. 34 (1) (2017) 266–272, https://doi.org/10.1007/s11814-016-0256-6.

[39] J. Kočik, A. Mance, A. Mihajlovič, The use of the potentiostat in the microstructural examination of uranium, J. Nucl. Mater. 37 (1970) 243–247, https://doi.org/10.1016/0022-3115(70)90089-9.

[40] N. Zaki, Electrocleaning, Met. Finish. 93 (1995) 125–130, https://doi.org/10.1016/0026-0576(95)93357-8.